www.czasopisma.pan.pl PAN www.journals.pan.pl

JOURNAL OF WATER AND LAND DEVELOPMENT

ISSN 1429–7426, e-ISSN 2083-4535

Polish Academy of Sciences (PAN), Committee on Agronomic Sciences
Section of Land Reclamation and Environmental Engineering in Agriculture
Institute of Technology and Life Sciences (ITP)

JOURNAL OF WATER AND LAND DEVELOPMENT
2020, No. 44 (I–III): 75–89
https://DOI.org/10.24425/jwld.2019.127048

Available (PDF): http://www.itp.edu.pl/wydawnictwo/journal; http://journals.pan.pl/jwld

Received 18.07.2018
Reviewed 27.10.2018
Accepted 20.12.2018

A – study design
B – data collection
C – statistical analysis
D – data interpretation
E – manuscript preparation
F – literature search

Failure simulation of Babar dam – Algeria and its impact on the valley downstream section

Aissam GAAGAI[1)], Abderrahmane BOUDOUKHA[2)], Lahcen BENAABIDATE[3)]

[1)] Scientific and Technical Research Center on Arid Regions (CRSTRA), Biskra, Algeria; e-mail: ✉ gaagai_aissam@hotmail.fr
[2)] University of Batna 2, Laboratory of Applied Research in Hydraulics, 05 078 Fesdis – Batna, Algeria; e-mail: boudoukha_abderrahmane@yahoo.fr
[3)] University of Sidi Mohammed Ben Abdellah, Faculty of Sciences and Technology, Laboratory of Functional Ecology and Environmental Engineering, Fez, Morocco; e-mail: lahcen.benaabidate@usmba.ac.ma

For citation: Gaagai A., Boudoukha A., Benaabidate L. 2020. Failure simulation of Babar dam – Algeria and its impact on the valley downstream section. Journal of Water and Land Development. No. 44 (I–III) p. 75–89. DOI: 10.24425/jwld.2019.127048.

Abstract

A failure analysis of Babar dam on the El Arab River was performed to highlight the impact of flood wave and velocities on the four villages downstream of the dam; Hella, Khérenne, Chebla and El Oueldja. The simulation of wave propagation along the El Arab River under several scenarios was performed by the hydraulic HEC-RAS model. This model is dedicated to the description of floods at the dam following a breach in the dike. The main factors considered in this simulation include the level of flood water, the flood hydrograph, and the typical scenario for this breach. The flood risk analysis revealed that the maximum of flood wave flow registered at the breach is (Q_{max} = 9253.02 $m^3 \cdot s^{-1}$), and is beginning to mitigate downstream of the dam along the El Arab River where it reached at the last village with a low flow (Q = 1110.64 $m^3 \cdot s^{-1}$). This simulation allowed drawing the risk map which showed the areas threatened by flood wave resulting from a total failure of the work, and consequently required a plan of security measures to moderate as much as possible the consequences of floods. A sensitivity analysis was conducted to approach the parameters of impact of the breach on the dam failure scenario. It was confirmed that these parameters as formulation time, breach width and side slope have a great influence on the dam failure scenario with the four adjustments (±20 and ±50).

Key words: *dam, dam failure, Hec-Ras, sensitivity analysis, simulation*

INTRODUCTION

All over world, several cities have been developed on along rivers, usually located downstream of different hydraulic structures such as dams and reservoirs. Such localization expose lives and properties to higher flood risk due to the potential failure of these structures example in Japan [SWANSON *et al.* 1986], Canada [CLAGUE *et al.* 1994], Malczyce (Poland) [CHALFEN *et al.* 2005] and Algeria [BERGHOUT *et al.* 2016; BOUCHEHED *et al.* 2017; BOUSSEKINE *et al.* 2016; DERDOUS *et al.* 2015]. To ensure good protection of these cities against devastating floods, practicing integrated management of flood risk at river basin remains necessary, and many projects have been implemented in recent years, to protect dams against problem of failure. Each dam failure resulted in damages to property and human lives. This study is based on the analysis of dam failure scenarios and their impact on the dam downstream. The fundamental tools for the protection of the valley downstream of dams relay on mitigating the damage caused by floods [BOUCHEHED *et al.* 2017; CHALFEN *et al.* 2005; MOKHTARI *et al.* 2016].

Several accidents have occurred worldwide, as in Oros, Brazil (1960), in Quebrada La Chapa (1963), in Cundinamarca in Colombia (1983), in Sunchon-Hyokin in South Korea (1961), in Limpopo in Mozambique (1977), in 1978 in Bakhera, Nepal (1978), in Morvi-Macchu (1979) and in Oressa, India (1980) and in the South Fork Dam, Pennsylvania, USA (1889) [MARCHE 2008]. Other dam failures included the Francis St Dam (California, 1928), Buffalo Creek Dam (West Virginia, 1972), Canyon Lake Dam (South Dakota, 1972), Teton Dam (Idaho, 1976), Kelly Barnes Dam (Georgia, 1977) and Lawn Lake Dam (Colorado, 1982) [ACKERMAN, BRUNNER 2012], and Algeria, as the dam Fergoug I, in 1881 that killed roughly 200 people in the Mascara region [SEMCHA *et al.* 2008]. This failure was caused by a flood of 850 $m^3 \cdot s^{-1}$. In the 20th century, about 200 dam failures causing a loss of over 8,000 lives and damage of several million euros recorded by [SINGH 1996]. Case studies show that dam failure can occur for different reasons. The US Hydrologic Engineering Center [USACE 1997] has issued a list of the most comprehensive causes: 1) earthquake; 2) landslide; 3) extreme storm; 4) the internal erosion; 5) equipment malfunction; 6) the damage of the structure; 7) the failure of the foundation; 8) sabotage. Quasi-whole failures start with a self-breach formation in an open overflow opening, opening itself internally by internal erosion. Basically, the breach is defined as the opening in the dam body which leads to the dam failure and this phenomenon causes the spread of concentrated water behind the dam towards the downstream zone [DINCERGOK 2007].

Some models are available to simulate the phenomenon of dam failure and the resulting wave of full spread downstream, such as HEC-RAS, WOLF 2D, MIKE, SOBEK and TELEMAC-2D. HEC-RAS was used in this study according to its universality and usability. This is a hydrodynamic dimensional model, led by USACE (Hydrologic Engineering Centers River Analysis System of the U.S. Army Corps of Engineers) [USACE 2010]. It's probably one of the one-dimensional models with greater use in the world, with the possibility of a variety of applications in the sediment transport simulation, the water temperature of modeling and, since 2003, simulation of the dam failure [HU, WALTON 2008].

This study aims to highlight the impact of a dam failure in semi-arid zone on the downstream part of the valley; case of Babar dam. The simulation of the failure was performed using the one-dimensional hydrodynamic model HEC-RAS. This one-dimensional hydrodynamic code is intended particularly to the study of rivers, canals and estuaries [MOKHTARI *et al.* 2016]. This model can simulate the breaking of a structure as a dam, or a lateral structure, as a dike. The objective of this study is to apply HEC-RAS to a scenario analysis of dam failure on the basis of given geometry data.

STUDY AREA

Babar dam is located at East of Algeria in the eastern reaches of the Saharan Atlas in the mountains of Nememcha (Figs. 1, 2). The downstream part of the valley is situated between two mountain ranges where are developed villages on edges of the watercourse such as Hella, Khérenne, Chebla and Oueldja. The frequent concentration of human activities in the nearby along the El Arab River, requires the care of problems caused by floods induced in the case of a partial or total failure of the dam, for the safety of this hydraulic structure against any hazards and, the safety of property and persons living downstream of the dam. Flood waves propagation produced by a dam failure, as experience shows, appear initially as dynamic waves by the predominant effect of inertia, then as a wave of continuity, as the flood subsides by moving downstream. The determination of wave propagation resulting from the breach must be able to predict their evolution in real time by using data stored upstream as the flood hydrograph in order to take appropriate protective. In case of exceptional flood resulting in a failure of the dike; the disaster is inevitable with loss of lives, properties and a negative impact on the environment (Figs. 2, 3).

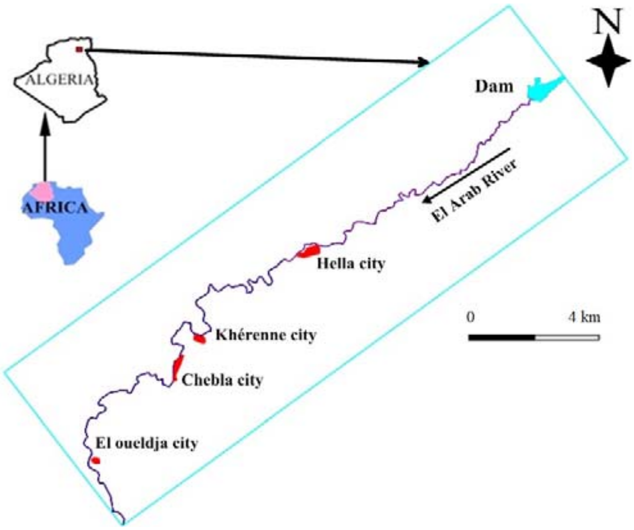

Fig. 1. Map of the study area; source: own elaboration

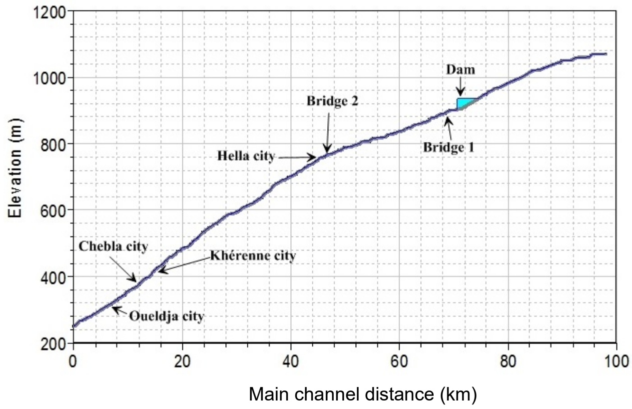

Fig. 2. Longitudinal profile of the El Arab River section near the dam; source: own elaboration

The dam was built on the El Arab River, which drains a watershed of 567 km^2. The rainfall recorded for 35 years (1970–2005) varies between 140 mm in 1970 and 563 mm in 2003 [GAAGAI 2009]. This dam is 37 m high, 1503 m wide. Its capacity is 41 mln m^3. The spillway is provided in a saddle which is located 650 m from the shoulder of the left bank and a width of 160 m. The region is subject to an irregular hydroclimatic regime as well on the seasonal as

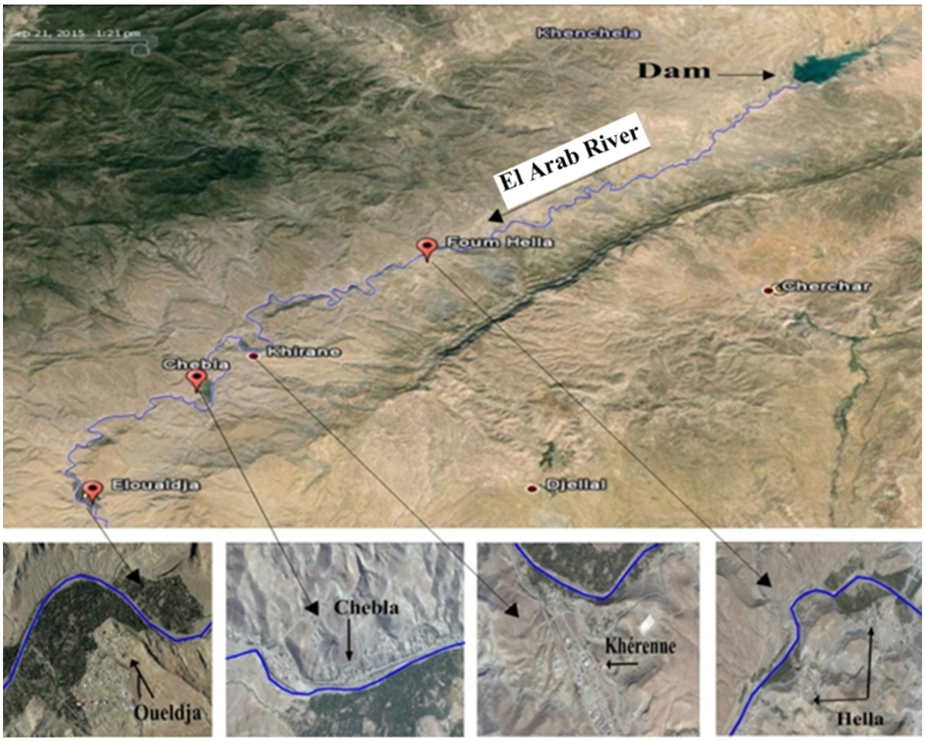

Fig. 3. Plan view of the dam and cities; source: own elaboration

on the interannual scale. This irregularity may have serious consequences on the status of the dam reserve and on the dam body security. The area can accommodate 60 mm in one day while the annual average is 300 mm. The restraint also receives a large share of annual liquid flows within a few days. The major part of the watershed (67%) is formed by Quaternary alluvium. The dam, built in 1990, consists of an earth dam with a clay core standing on waterproof green Danian marl.

In the face of the climate change that struck this region where there was really very dangerous exceptional floods, and in particular the oversized of the flood spillways work which cannot withstand this flood. All this can threaten the body of the dam with a possible rupture. Therefore, the dam is threatened by two risks, the first is natural (exceptional flood) and the second risk is human (sizing study the work of the spillway is poorly done).

MATERIALS AND METHODS

HYDRAULIC MODELING

The Saint-Venant's model is the most used for performing modeling in an unsteady flow regime with free surface [SIRABAHENDA 2012]. There are several methods of discretization of Saint-Venant's equations of which the most widely used are the finite differences method, the finite volumes method and the finite elements method, the resolution strategy. The choice of initial conditions and boundary conditions may condition the stability, accuracy and speed of convergence of the digital solution [ANCY 2010]. The digital resolution of Saint-Venant's equations in the HEC-RAS 4.1 software uses the finite differences implicit scheme based on linearization technique developed by Preissmann [LIGGETT, CUNGE 1975]. The HEC-RAS model 4.1 uses the equations derived by BARKAU [1982] to calculate the unsteady flow from the concept of flow separation in minor riverbed and flood plains initially proposed by SMITH [1978].

HEC-RAS 4.1 MODEL

HEC-RAS is the software that allows to perform calculations of both steady and unsteady river flow, sediment carryover capacity, steady flow calculations and analysis of water temperature. The elaboration of an HEC-RAS hydraulic model requires an accurate representation of field data and hydrological inputs used as boundary conditions. This software is able of modelling hydraulic works in a section of water stream. It allows making cross sections with a variable Manning coefficient, to differentiate active and non-active zones in a canal and to create interpolated cross sections. Given the dynamic nature of flood wave produced by a dam failure, as well as the size and geometry of the reservoir, the calculation of the unstable flow of water surface profile was used for the dam-breach scenario.

The calculation of unstable flow for the HEC-RAS model can simulate both under-critical and super-critical flows that were produced in the simulations. For most simulated sections, the under-critical flow, the flow velocity being slower than the propagation wave velocity; however, the super-critical; higher velocity flow than the propagation wave velocity was likely to occur at the dam failure location.

OPERATION AND APPLICATION OF HEC-RAS 4.1

Detailed information of the ground of the main canal and floodplains are the important required data to create a hydraulic model of the river. For modelling dam failure, the size of breach and the timing of the breach are required. This section of document deals with the extensive data given to develop a river hydraulic model for the dam failure analysis. The cross section data can be modified to match the reservoir volume-curve elevation. This can be achieved by performing a series of dam regular flow profiles at the upstream end of the reservoir with a low flow and altering the initial condition downstream for reservoir various elevations. Database requirements to calculate flow in HEC-RAS are described below.

Geometric system arrangement

The dam failure study along the river (98 km) downstream from dam site was channelled by a total of 176 sections located at an average distance of about (500–1000 m). Figure 4 covers an area from 30 km before dam's site, until the Oueldja town. The cross sections were obtained from a surface in a triangulated irregular network form, topographic mapping created using the Digital Elevation Module (DEM) processed data using 3D Civil Autocad software. 1300 additional sections were interpolated in HEC-RAS to improve calculation stability. Four villages represent the essential part in the impact assessment and a total of two bridges have been included in the model. The bridges were modeled as hydraulic structures whenever the necessary data were available. The Figure 4 shows a set of 176 cross-sections used for the selected dam failure model. They correspond to cross sections spaced at intervals of 0.5 km throughout the studied sections and locations of towns within the model.

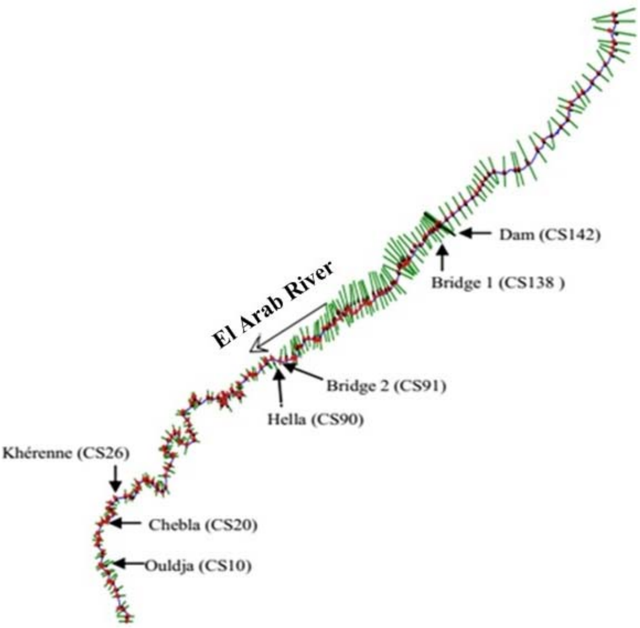

Fig. 4. The El Arab River and sections; source: own elaboration

Hydraulic data

Turbulent flow model requires a minimum of two hydraulic forms, energy loss coefficients (Manning coefficient), and turbulent flow boundaries conditions. The identification of the bed roughness coefficient and different ranges river sides have been performed using the river's geometry, the vegetation on the river bed sides and the amount of the bed material, they represent the form of two types of roughness coefficient which have been chosen according to the output on the ground, where the main channels have been found to consist of some stones and weeds. However, the plains are represented by medium to dense brush, in winter and undergrowth, flow below branches which are 0.0365 on the main channels and 0.1 on the left and right banks.

Boundaries conditions must be established within all open ends for simulated river water. In this study, the boundary conditions are used in the digital model: the upstream reservoir flow hydrograph shown in Figure 5 is used to define the upstream boundary condition. This condition used in the digital model is a natural slope between the last two sections of the river. For the initial condition, the reservoir average daily output was 31 $m^3 \cdot s^{-1}$. This flow was estimated at initial influx and at dam outlet.

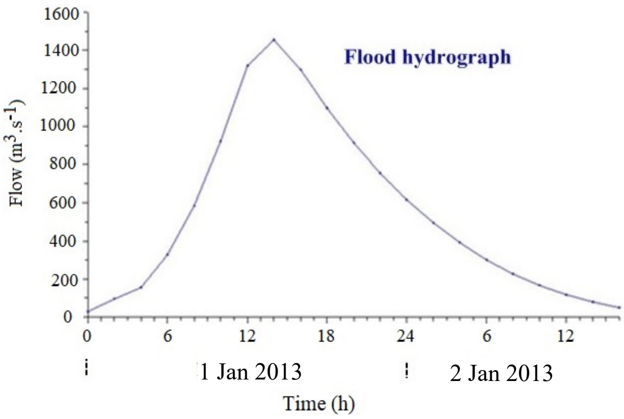

Fig. 5. Dam inlet flood hydrograph; source: own elaboration

BREACH PARAMETERS ASSESSMENT

The description of the breach shape in HEC-RAS focuses on the calculation effort of the delivery flood hydrograph at the breaching outlet. Breach, in embankment dams, is generally assumed to be trapezoidal, so that the shape and size of the breach is defined by the breach height, the breach average width, a width tilt angle (slopes) and breach formation time. These values represent the maximum breach size [MICHAEL 2010]. A general diagram showing the breach is shown in Figure 6. In order to perform a simulation of the flood wave propagation after a dam failure, all parameters must be assessed and provided as inputs to the dam failure. For prediction of breach parameters, many researchers have proposed simplified methods for predicting the output peaks of a built dike [MARCHE 2004]. These methods are used at the level of

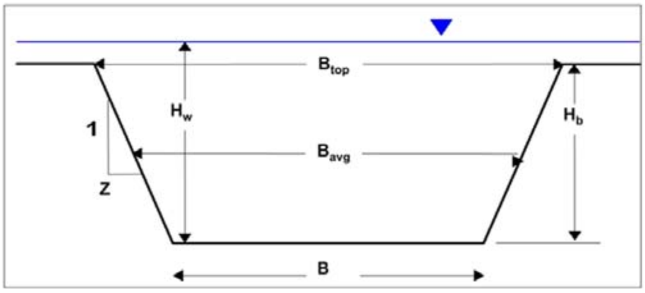

Fig. 6. Breach profile type; source: own elaboration

recognition and ascertain the reasonableness of a dam failure and flow hydrograph to develop the breach parameter estimation. This work focuses on the interpretation and application of results of these methods for modelling failures with the HEC-RAS model. Several authors have carried out studies on real cases and found that the most common breach form is the trapeze. For example, WAHL [1998] used a lot of relationships available for predicting the breach parameters of 108 documented cases studied and indicated the predictions on the observed values. In this investigation, we have chosen three methods of calculation based on their use for several dam safety monitoring, to size the breach according to FROEHLICH [1995a] (Eqs. 1 and 2) according to MACDONALD and LANGRIDE-MONOPOLIS [1984] (Eqs. 3 and 5) and that of VON THUN and GILLETTE [1990] (Eqs. 6 and 7).

$$B_{\mathrm{ave}} = 0.1803 K_0 V_w^{0.32} h_b^{0.19} \tag{1}$$

$$t_f = 0.00254 V_w^{0.53} h_b^{-0.9} \tag{2}$$

$$V_{\mathrm{eroded}} = 0.00348 (V_{\mathrm{out}} h_w)^{0.852} \tag{3}$$

$$t_f = 0.0179 (V_{\mathrm{eroded}})^{0.364} \tag{4}$$

$$B = \frac{V_{\mathrm{eroded}} - h_b^2 (C Z_b + \frac{h_b Z_b Z_3}{3})}{h_b (C + \frac{h_b Z_3}{2})} \tag{5}$$

$$B_{\mathrm{ave}} = 2.5 h_w + C_b \tag{6}$$

$$t_f = \frac{B_{\mathrm{ave}}}{4 h_w} \tag{7}$$

The maximum flow is provided by the following formula:

$$Q_p = 0.607 V_w^{0.295} h_w^{1.24} \tag{8}$$

Where: B_{ave} = average width (m); h_w = depth of water above the bottom of the breach (m); h_b = height from the top of the dam to bottom of breach (m); Z = breach embankment slope (m); B = lower width (m); t_f = breach formation time (h); V_w = reservoir volume at time of failure (m^3); K_0 = constant (1.3 for overtopping failures, 1.0 for piping); V_{eroded} = volume of material eroded from the dam embankment (m^3); V_{out} = volume of water that passes through the breach (m^3); C = crest width of the top of dam (m); $z_3 = z_1 + z_2$; z_1 = average slope (z_1:1) of the upstream face of dam; z_2 = average slope (z_2:1) of the downstream face of dam; z_b = side slopes of the breach (z_b:1) 0.5 for the MacDonald method; C_b = coefficient, which is a function of reservoir size, see Table 1.

Table 1. The coefficient C_b dependent on the reservoir size

Reservoir size (m^3)	C_b (m)
<1.23·10^6	6.1
1.23·10^6–6.17·10^6	18.3
6.17·10^6–1.23·10^7	42.7
>1.23·10^7	54.9

Source: own elaboration.

We have performed two different simulations using each of these formulas:
- compare the maximum outflow of the breach with the one given by the empirical formulas;
- choose the simulation which will be used in completion of the flood map.

RESULTS AND DISCUSSIONS

SCENARIO OF DAM BREACH FAILURE

The three quantitative analysis methods are used to predict the breach parameters in dam embankment and breach outflows such as width of the breach and breaking time. The peak flows are quite important for the three methods. The breach parameters calculation by the three methods of Froehlich, von Thun and Gillette and MacDonald and Langridge-Monopolis are respectively of average width of the breach having generally 136.82 m, 147.4 m and 147.2 m. The breach time formation for Froehlich (1.06 h), for von Thun and Gillette (0.99 h) and for MacDonald and Langridge-Monopolis (1.604 h). The peak flow calculated after simulation of each formula also includes 9253.02 m^3·s^{-1} for Froehlich, 10286.13 m^3·s^{-1} for von Thun and Gillette and 7099.42 m^3·s^{-1} for MacDonald and Langridge-Monopolis (Tab. 2, Fig. 7). Application of the three formulas allows having results relatively close. Analysis of these results shows that flows issued from the breach are very close with average flow obtained by empiric formula 9566.62 m^3·s^{-1}. The proposed relationship by MACDONALD and LANGRIDE-MONOPOLIS [1984], VON THUN and GILLETTE [1990] and FROEHLICH [1995a] have been brought up earlier in this investigation. Table 2 compares number of studied cases, widths and breakage flows observed for each of these relationships, by using cases study data based on real data. MacDonald and Langridge-Monopolis used 42 of these cases to develop their relationship, von Thun and Gillette used 57 of these cases: Froehlich used 63 of these cases. Globally, it seems that formula of Froehlich can supply reasonable estimations of the upper limit of peak outflow. For this application, results of Froehlich's method were considered as the best estimation of flow outlet peak. However, we can adopt it since the formula of Froehlich is the most adapted to earth dams, the most recent and it is determined from investigations of numerous real cases (63 cases) [WAHL 2004] by contrast, other formulas represent a preliminary estimation. Consequently, we cannot adopt it for a complete study.

Obtained results by the application of HEC-RAS model have been comforting because they become in the range of the values obtained from the basic of methods regression. However, in the same time, they also stated that even

Table 2. Flowrate simulation results by HEC-RAS Code

Formula of	Number of cases studied	B	B_{ave}	B_{top}	Z	t_f (h)	Q_{max} ($m^3 \cdot s^{-1}$)
		(m)					
MacDonald and Langridge-Monopolis	42	105.60	147.20	188.9	0.9	1.604	7 099.42
Von Thunand Gillette	57	93.80	147.40	201.0	0.7	0.990	10 286.13
Froehlich	63	75.16	136.82	198.5	0.6	1.060	9 253.02

Explanations: B = lower width, B_{ave} = average width, B_{top} = top width, t_f = breach formation time.
Source: own elaboration.

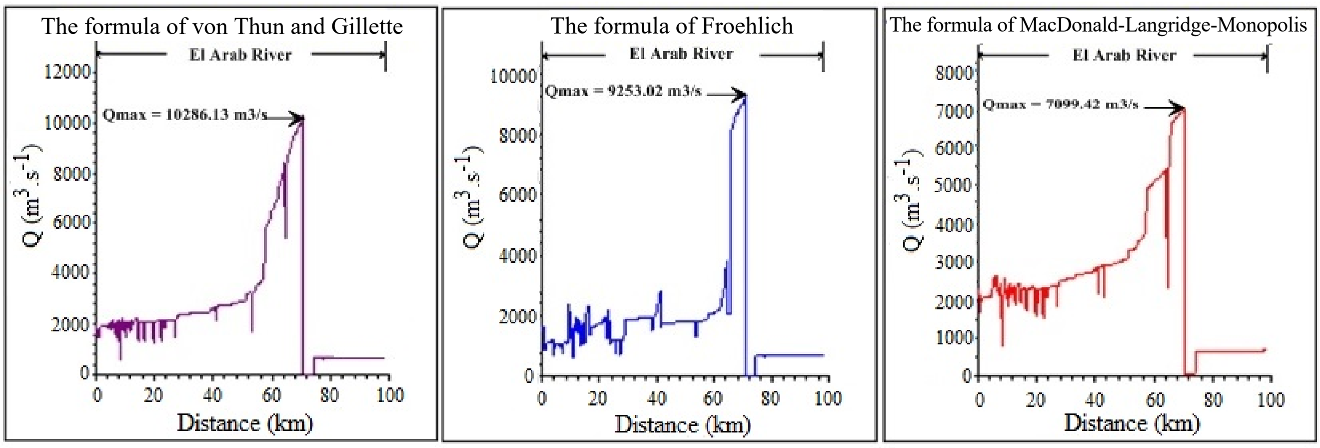

Fig. 7. The evolution of the flood wave by the three empirical methods; source: own study

methods based on physics can be highly sensitive to analysis the hypothesis concerning breach morphology and development position of the initial breach. Application of this analysis by HEC-RAS's model thanks to these breach forecasting methods, demonstrated possibility to limit breakage mechanism which has not been revealed. This breach parameter analysis used a data base on failure of numerous dams shows that significant judgement analysis should be exerted in interpreting the breach forecasting parameters.

FLOOD WAVE EVOLUTION

Flood hydrograph at level of the breach outlet calculated from the dam is represented on Figure 8. It highlights that after about 30 minutes of dam's failure, the outflow peak is (9253.02 $m^3 \cdot s^{-1}$) and then, it begins to mitigate until a 124.53 $m^3 \cdot s^{-1}$ after about 2:15 h from dam's breakage, where the reservoir will be empty and the total volume will flow into the river and, this means that a volume of $41 \cdot 10^6$ m^3 (minimum) will be conveyed towards the dam downstream in very short duration of 2:15 h. This situation is traduced by important consequences from this flood wave. Flood hydrograph shows that reservoir and dam's body have been exhausted at the time end simulation. These serious changes in the dam breach characteristics and the geometrical parameters existing in river downstream have generated a significant increase in peak flows on the dam dyke and downstream area. The peak flow of different sections is not uniform to the dam downstream. This observation shows that peak flows were sensitive to change of the breach lateral slope, Manning coefficient and particularly the El Arab River geometry bed at different degrees for limiting failure in time.

FLOW EVOLUTION/FLOOD WAVE VELOCITY

Failure wave propagation investigation was conducted on over 75 km in the El Arab River valley. Taking into account the specificity of this dam linked at its superficial watershed 567 km^2, a progressive failure has been simulated at the dam downstream. After failure, the flow spatial evolution along the El Arab River recorded a peak of 9253.02 $m^3 \cdot s^{-1}$ just after few minutes of the dam failure, and then it begins to mitigate far of the dam where it reaches the last village (Oueldja) with a value of 1110.64 $m^3 \cdot s^{-1}$. This evolution can give a picture on the importance of this flood wave and consequences which can be generated at the dam downstream and particularly with these factors (longitudinal profile slope of the river, geometry and ground type of this area) which have a supporting role at this flood wave spreading quickly towards downstream. According to results obtained by HEC-RAS model, the three elements such as max flow (Q_{max} = 9253.02 $m^3 \cdot s^{-1}$), exhausting time of the dam reservoir (t = 2:15 h) and volume of the dam reservoir ($V = 41 \cdot 10^6$ m^3), show that the dam failure may constitute a real hazard for all villages and infrastructures as well for population living downstream of the dam. It is about area within an upper water level elevation known to severe flooding (Tab. 3). Figures 9 and 10 represent respectively the peak flow in $m^3 \cdot s^{-1}$ after the dam failure and, the velocity variation of maximal flows reached in $m \cdot s^{-1}$.

The flow velocity is part in calculation of the impact on structures. It shows the violence of flow and contributes to movement quantity estimation based on numerical modelling of Saint Venant's equation. In these equation, velocity and water height are unknown. Flow velocities are very important and can generate serious damages even

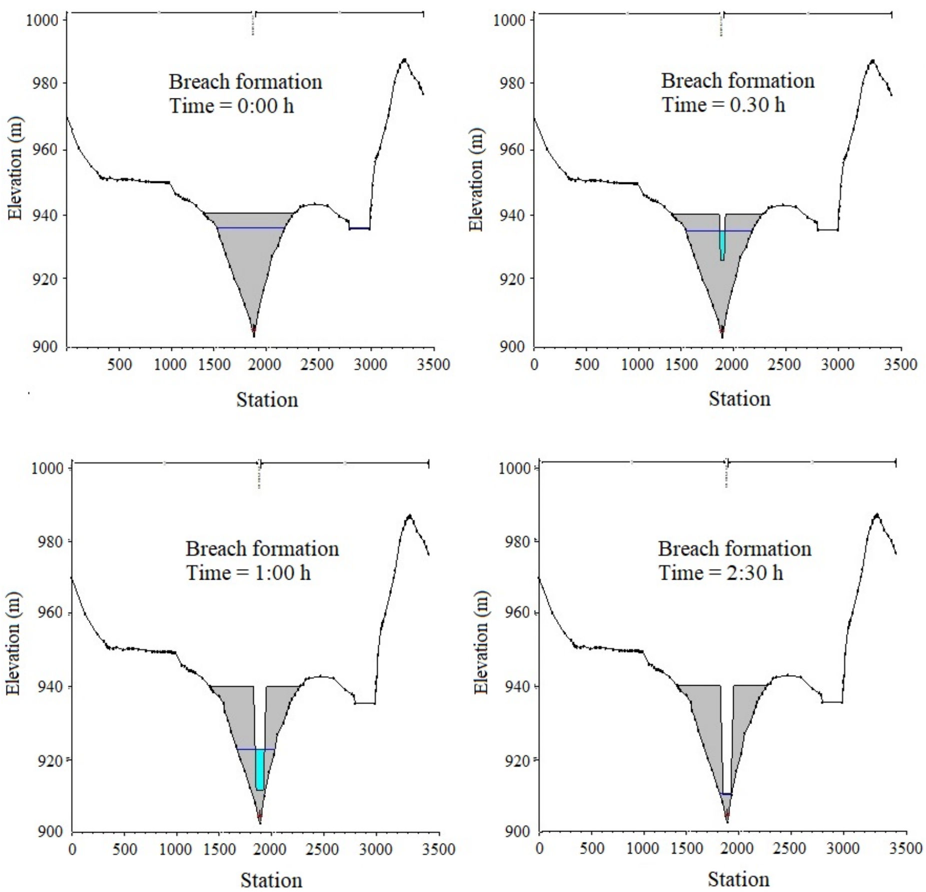

Fig. 8. Dam failure and formation breach in time; source: own study

Table 3. Simulated flood wave propagation downstream of the dam

Station	Section	Profile	Q_{max} ($m^3 \cdot s^{-1}$)	Minimum main channel elevation (m)	Water surface elevation (m)	Energy gradeline elevation (m)	Energy gradeline slope	Velocity ($m \cdot s^{-1}$)	Flow area (m^2)	Width (m)	Arrival time (h)	Height of water (m)	Froude
Bridge 1	138	Max WS	**8 989.01**	900.00	911.07	913.24	0.008019	**11.97**	2 471.60	399.52	**00 :15**	**11.07**	1.16
Bridge 2	91	Max WS	**1 805.89**	760.71	766.77	767.28	0.004337	**5.39**	1 014.20	323.47	**06 :40**	**6.06**	0.75
Hella	90	Max WS	**1 804.56**	757.00	762.09	762.67	0.007279	**5.67**	943.87	399.65	**06 :45**	**5.09**	0.92
Khérenne	26	Max WS	**1 458.34**	392.73	401.66	402.31	0.002000	**4.69**	731.92	154.64	**07 :45**	**8.93**	0.54
Chebla	20	Max WS	**1 395.65**	357.22	364.08	364.32	0.001404	**3.15**	1 065.10	269.09	**08 :00**	**6.86**	0.43
Oueldja	10	Max WS	**1 110.64**	305.23	310.43	311.66	0.010100	**6.03**	525.30	476.63	**08 :45**	**5.20**	1.06

Source: own study.

with a weak water height. The simulated flood wave propagation in the dam downstream, demonstrates unstable and irregular variation of the flow velocity after the dam failure. This variation depends mainly on geometry of the rugged valley along of the El Arab River and the river slope (Tab. 3, Fig. 10). According to results obtained from simulation by HEC-RAS software, flood wave allowed to form, in the dyke, a very large breach surging downstream with high velocities. According to velocity curve appearing on the schemes below, the velocity of a peak flood wave may reach values nearly of 26.5 $m \cdot s^{-1}$, which begins to mitigate from 27 km of the dam (Fig. 10).

Spatial evolution of flood wave velocity recorded three peaks in three different stations: peak 1: station no. 75.125, $V = 19.10\ m \cdot s^{-1}$, peak 2: station no. 27.1666, $V = 26.5\ m \cdot s^{-1}$ and peak 3: station no. 15.5, $V = 19.02\ m \cdot s^{-1}$. This evolution is approved by the Figures 11 and 12 which respectively represent shear stress of the bed of the El Arab River, and water flow power during flood wave propagation at the dam downstream. It has been noted that the spatial variation of flood wave velocity is similar to two factor; the shear stress factor and bed transporting of the El Arab River and, water flow power factor which has been determined according to soil type, geometry and particularly with steep slopes of the river, which showed that the velocity peaks recorded in this investigation are essentially due to soil type and to the river steepened slopes. According to Figure 10, the spatial variation of flood wave velocity appears in a random manner which is due to rough ground geometry of the El Arab River valley located between Aures and Nememcha outcrops.

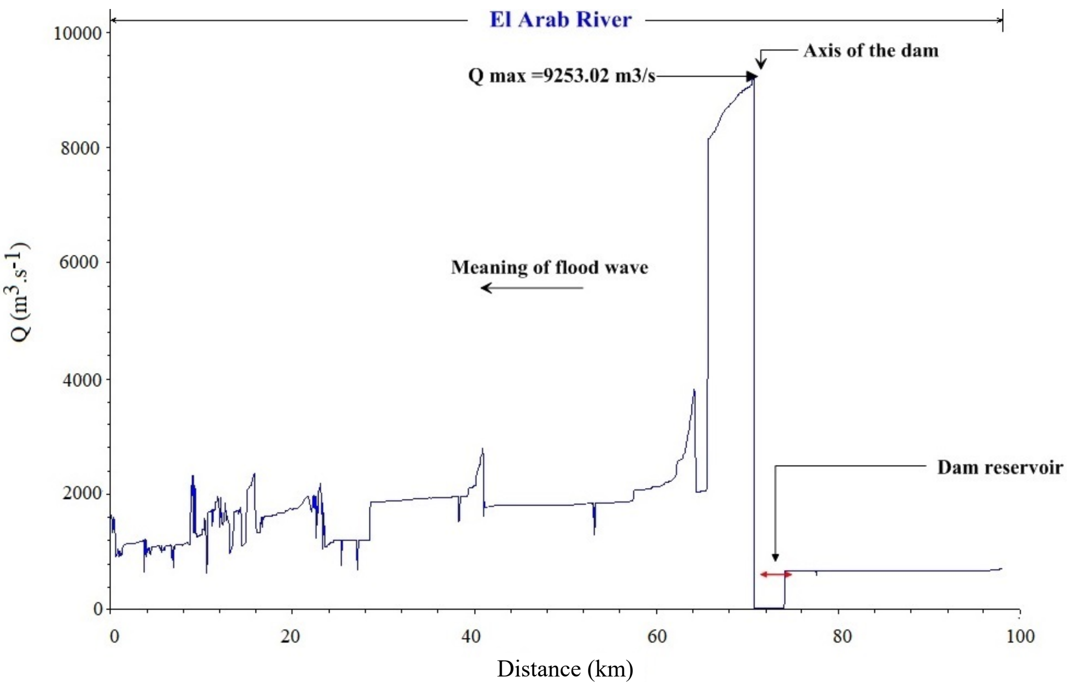

Fig. 9. Variation in flowrate after dam's failure; source: own study

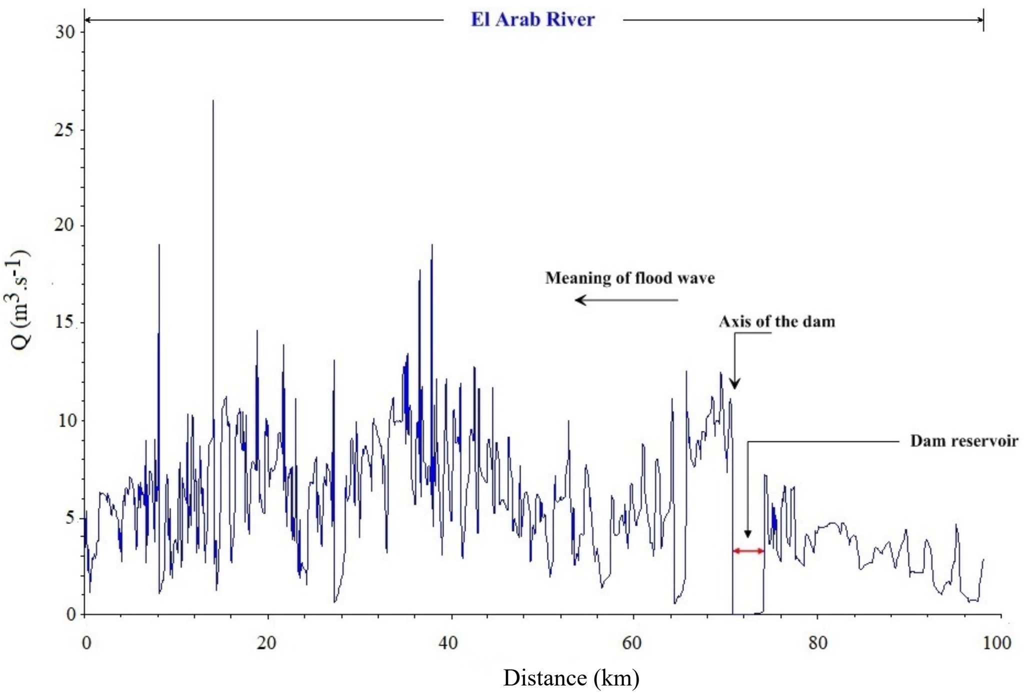

Fig. 10. Variation in flood wave velocity after dam failure; source: own study

PROFILE OF MAXIMUM WATER SURFACES

The profile surface of the flood wave with maximum levels estimated by HEC-RAS model on the totality of the El Arab River following Baba dam failure is shown in Figure 13. The first peak is represented by the dam reservoir surface just some seconds after the failure. The two other peaks are linked to valleys with shallow slopes as plain of Hella village. Adversely, the remaining flood wave surface profiles represent very narrow and very rugged valleys. According to results obtained by HEC-RAS model, water levels variation in this area presents an important fluctuation along the El Arab River.

FLOOD RISK ANALYSIS

The propagation wave simulation at the dam downstream by this hydrodynamic one-dimensional HEC-RAS model, let predicting a dam failure in the near future with a very dangerous flood wave for areas located at downstream of the dam, notably which they are at the edge of the El Arab River. The flood coming from the dam breach

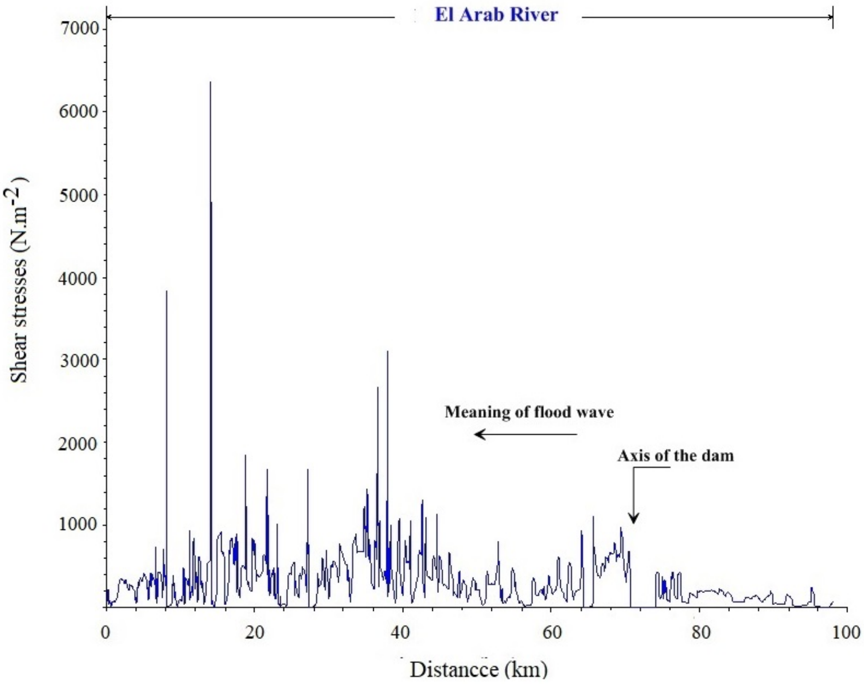

Fig. 11. Shear stress and the transport of the bed of the El Arab River; source: own study

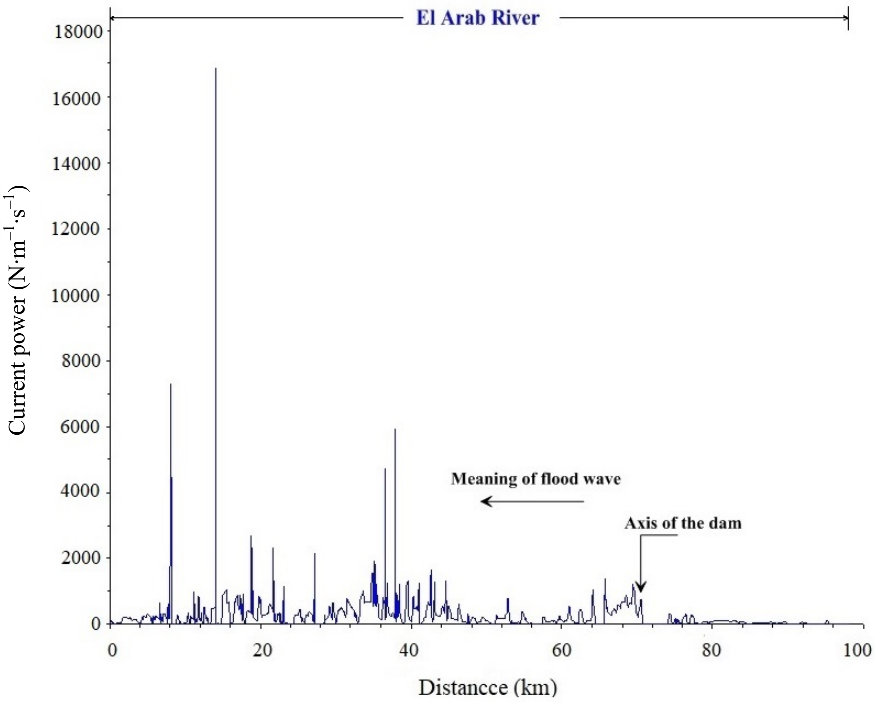

Fig. 12. Water current power of the flood wave; source: own study

with a flow of 9253.02 $m^3 \cdot s^{-1}$ constitutes a permanent danger on the investigated area, becoming exposed to this submersion wave (Fig. 14). This wave can reach the first bridge opening of (3×3 m) (section 138) located at distance of 903 m of dam axis with a flow of 8989.01 $m \cdot s^{-1}$ and water height equal to 11.07 m in a very short time of 0.20 h (Fig. 15). Bridge will be unavoidably submerged and totally damaged and consequently breaks road linking Babar town to other villages (Hella, Khérenne, Chebla and Ouldja) located at downstream of the dam. The road network is an important factor in economic and social development which also be managed by taking into account the failure risk of a dam dyke. Currently, our life is developing by implementation of projects which need human and material resources that provoke displacements of important populations. However, in order to avoid roads break risk, it is necessary to enforce communication protocols with authorities in case of emergency. The second stream crossing

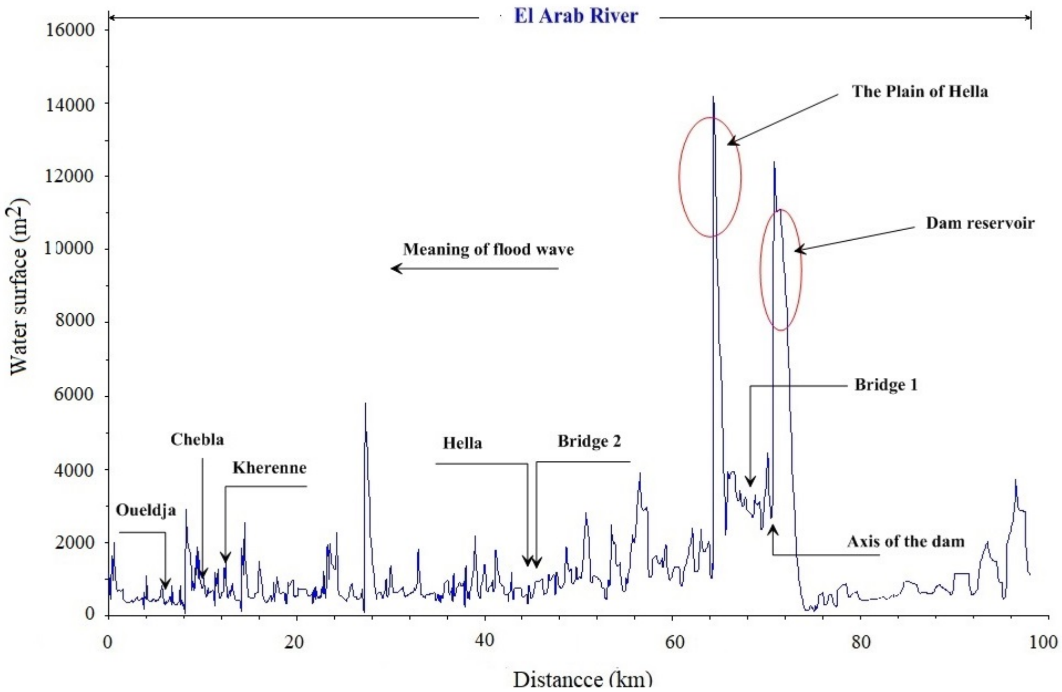

Fig. 13. The surface of the water during the flood; source: own study

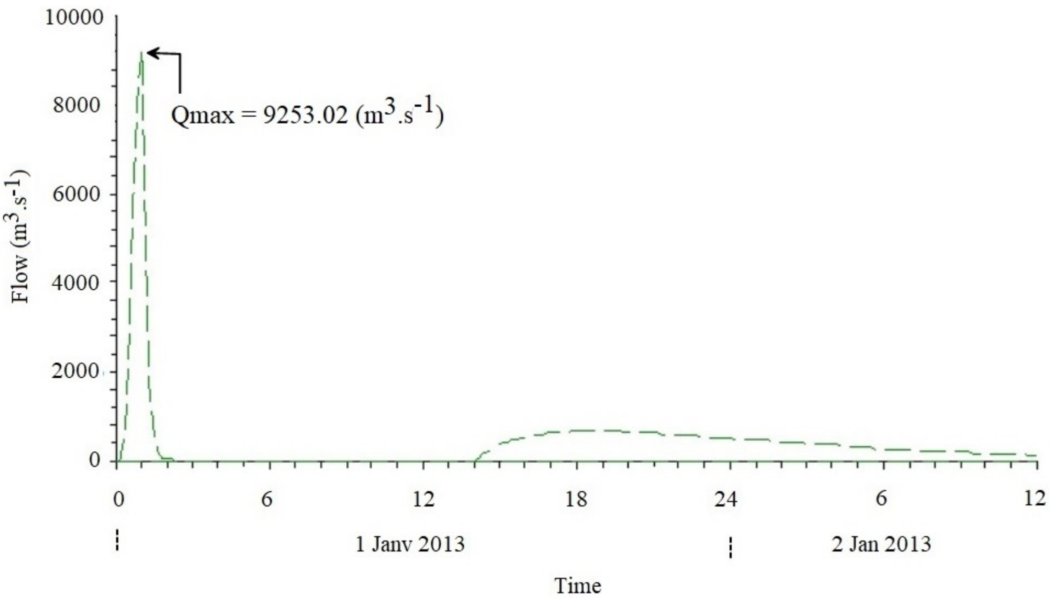

Fig. 14. Breach hydrographs at dam; source: own study

by a bridge (section 91) is located at distance of 18.50 km of the dam axis at the entrance of Hella village. The propagation wave arrived at level of the bridge in time of 6.40 h with a flow of 1805.89 $m^3 \cdot s^{-1}$ and with a water height of 6.06 m (Fig. 15a). Village of Hella is the first exposed to such flood (section 90) with a flow of 1804.56 $m^3 \cdot s^{-1}$, and a water height of 5.09 m in time of 6.45 h (Fig. 15c). This wave with such flow will submerge a part of Hella village and will have a severe and destructive impact. The second bridge located at downstream of Hella village (section 89) will also be damaged by the flood wave and that do not allow evacuating population of the river left bank towards Nemamcha Mountain.

The second village of Khérenne (section 26) is located at 29.83 km (as the crow flies) from the dam axis. Submersion wave will reach this village in a time of 7.45 h with a flow of 1458.34 $m^3 \cdot s^{-1}$ and a water height of 8.93 m (Fig. 15d). As well as for Hella village, Khérenne village will be reached in part by this flood wave which will floods the agricultural lands located in the right bank of the river.

The third village of Chebla (section 20) is located downstream at 32.90 km of dam axis (as the crow flies). The flood wave will reach the village in time of 08.00 hours with a flow of 1395.65 $m^3 \cdot s^{-1}$ and a water height of 6.86 m. Due to topographical morphology which is similar with the Khérenne village, the Chebla village (Fig. 15e)

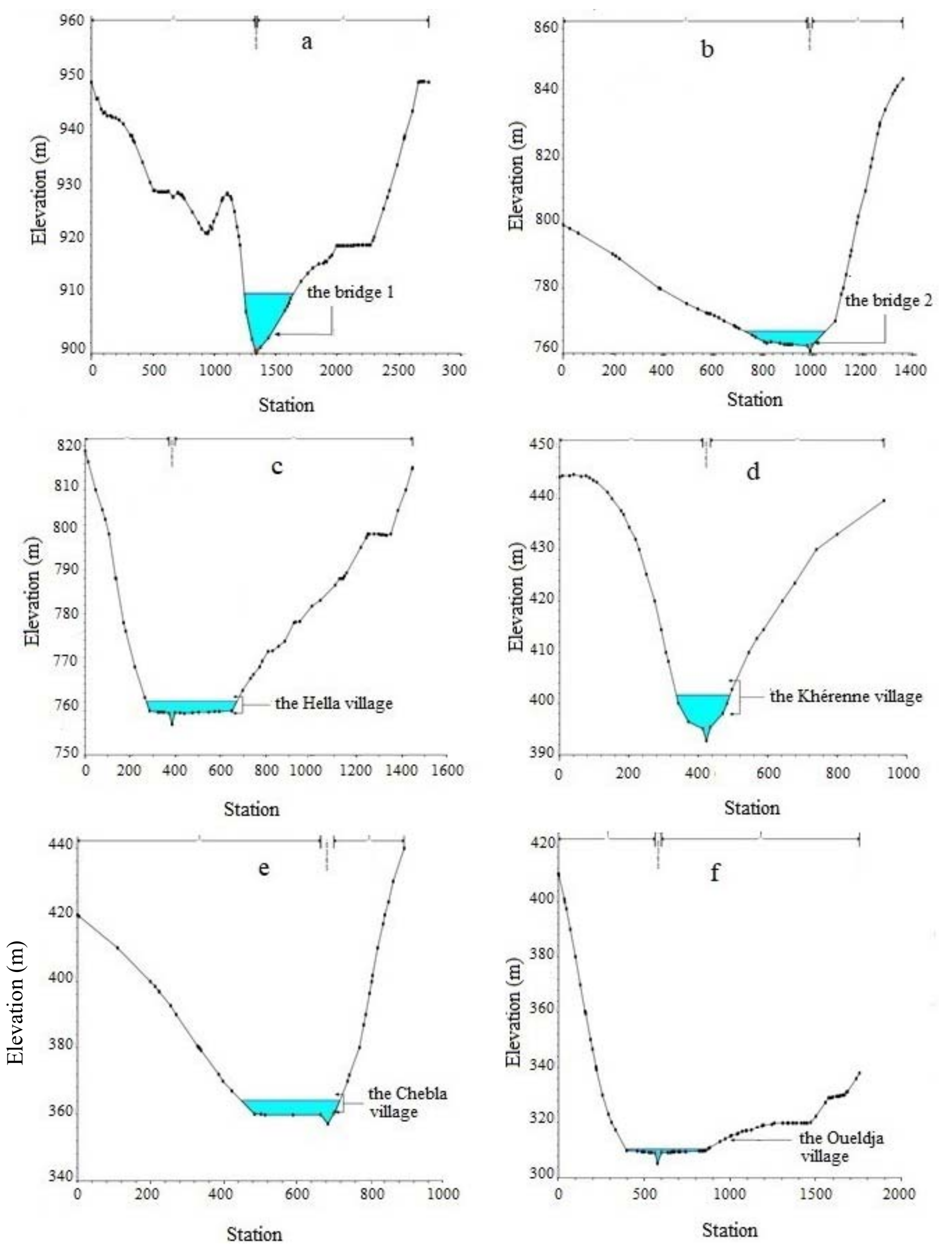

Fig. 15. The water level after the failure at: a) the bridge 1, b) the bridge 2, c) the Hella village, d) the Khérenne village, e) the Chebla village, f) the Oueldja village; source: own study

will face the same consequences of the flood wave on the village and agricultural yards. The last village of Oueldja (Fig. 15f) (section 10) is located at 41.4 m of dam axis (as the crow flies). According to Figure 16, the flood wave with a flow of 1110.64 $m^3 \cdot s^{-1}$ has no effect on this village, which is higher of 8 m compared to the El Arab River bed, while the flood wave height has only 5.2 m.

According to the HEC-RAS simulation, in failure case of the dam, the propagation wave can generate human, material and property losses with disastrous consequences on environment until village Oueldja. The position of villages located downstream of the dam and at the edge of watercourses, delineated by watersheds of the two mountain ranges, favourites the orientation of flood wave towards downstream, and do not allow capping the flood. This dam dyke failure causes the generation of a submersion wave which brutally raises water level towards downstream. The Risk Map represents the areas threatened by the submersion wave which would result of a total breakage of the work (Fig. 16). This flood will flow along a large part of the villages located downstream of dam and will destroy a wide part of the road and agricultural lands. This simulation allows concluding that villages of Hella, Khérenne and Chebla are seriously exposed to the flood wave, while village of Oueldja is totally protected in case of a dam breakage.

The dam failure investigation analysis allows us demonstrating that the failure phenomenon would be very dangerous and devastating on the areas downstream of the dam. According to the risk map established using HEC-RAS model, an integrated strategy of flood waves management at downstream of the dam in case of dam breakage should be implemented to save as much as possible villages located on the river bed by using the risk map, It is

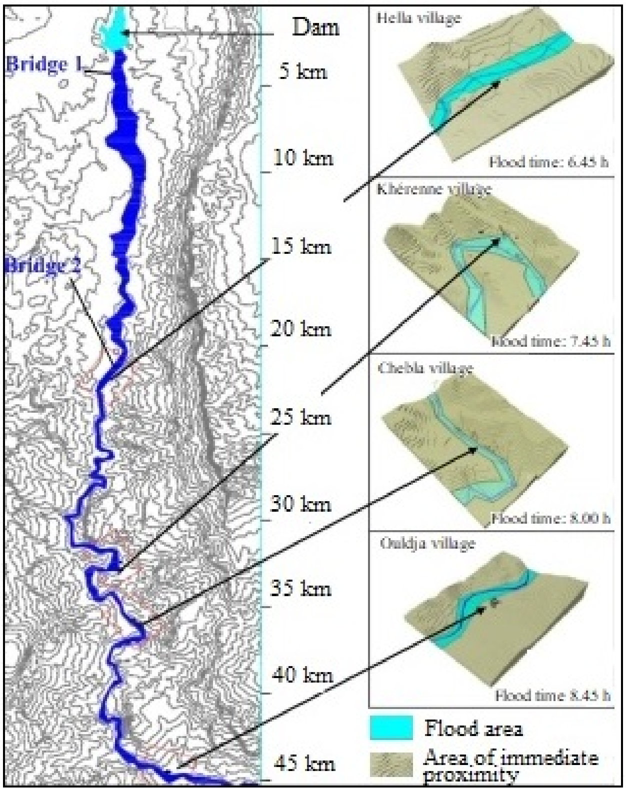

Fig. 16. Map of flooding by dam failure Babar; source: own study

noted that the first villages (Hella, Khérenne and Chebla) are the most exposed to this submersion wave notably villages of Hella and Chebla (Fig. 16). So we have an obligation to make available to the authorities a wide ranging of measures to attempt mitigating flooding of these villages in case of dam's failure. It will be indispensable to maintain the proper functioning of the dam and an early warning system, also to establish an effective and rapid emergency evacuation plan of riparian, before the arrival of the flood wave. This flood risk analysis by this hydraulic model allows assessing the necessary time for submersion wave to reach the villages. According to the simulated breach formation time (1.06 h), and the propagation time of the flood wave downstream of the dam, the first village will be reached by the flood wave within 6.45 h and the last village within 8.45 h, which allows implementing the warning plan with more or less effective manner (Tab. 3).

SENSITIVITY ANALYSIS

The sensitivity analysis is an efficient tool to identify how parameters variation of calculation code input contribute qualitatively or quantitatively to the output variation so, sensitivity analysis can help to validate, simplify or better understand a model for guiding the efforts of the input parameters characterisation [SIMON 2015]. Sensitivity analysis is used in this study to obtain an overall evaluation on the accuracy of the model HEC-RAS when it is used for analysing the dam failure impact for alternative scenarios, and so for general information detailed concerning the importance of interactions between breach formation parameters in case of failure. A method based on variance assumes a probability distribution for taking into account the uncertainty on input parameters. Regarding sensitivity analysis, a study of the sensitivity results is presented to different parameters and this for different scenarios of failure. We also are looking for evaluation of the influence of each parameter on failure evolution of the dam for each scenario. For this purpose, the sensitivity coefficient was calculated which corresponds to the difference between the added value (±20 and ±50) and the initial value, for each parameter evaluating the flood wave variation generated by an increase or decrease of the studied parameter unit.

Breach parameters impact on dam's failure scenario. This analysis is made to assess the impact of all parameters on the model results. It is about of three breach parameters that influence the dam failure scenario and are composed of the breach formation time, width of the breach and the breach depth. In this investigation, 12 simulations have been performed for the dam failure scenarios with three parameters and each parameter with four adjustments (±20 and ±50). The sensitivity analysis of the dam failure is summarized in Tables 4 and 5. These tables represent the sensitivity analysis of the dam failure with two scenarios which were compared to four different spots (villages of Hella, Khérenne, Chebla and Oueldja). We noted that there is a significant change with all scenarios and all parameter adjustments corresponding to this simulation, such as the adjusted full formulation time, the adjusted breach width and the adjusted breach depth on three dimensions representing the flood wave; the height, the velocity and the width of flood wave for each identified location.

Table 4 summarizes the dam break sensitivity analysis 1 (±20%) and, two scenarios are compared at the four villages. There is significant difference among the "break without adjustment", "adjusted full formulation time", "adjusted breach width" and "adjusted breach depth" in height (m), width (m) and velocity at each identified location.

However, the flood wave width of the breach formation time adjustment is important than the height and velocity of this flood wave. It sounds that there exists a critical set of breach parameters corresponding to a "width of flood wave".

Table 4 also shows that the height (m) is not so sensitive to the adjustments of the given breach parameters within ±20%. Only in the case of adjusted full formulation time in ±20% the height is important without Adjustment.

Table 5 highlights the dam break sensitivity analysis 2 (±50%) and significant change is observed either. However, besides the slight change in the scenario of "adjusted breach depth" for the velocity ($m \cdot s^{-1}$) and height (m) in ±50%, further new information is given in Table 5 as compared with Table 4. For Babar dam break analysis, the height to the flood wave is insensitive to the change of the given dam breach parameters.

This sensitivity analysis of the dam failure with the four adjustments (±20 and ±50) for each parameter such as the adjusted breach formation time, the adjusted breach width and the adjusted breach depth reveal significant changes of flood wave with these dimensions for velocity

Table 4. Dam break sensitivity analysis 1 (±20%)

Breach parameters	Flood parameters	Adjustments (±20%)	Hella	Khérenne	Chebla	Oueldja
Adjusted breach depth	width (m)	decrease –20%	399.65	152.52	265.13	475.72
		break without adjustment	399.65	154.64	269.09	476.63
		increase +20%	399.77	157.28	264.49	475.49
	velocity ($m \cdot s^{-1}$)	decrease –20%	5.67	5.02	2.54	5.99
		break without adjustment	5.67	4.69	3.15	6.03
		increase +20%	5.68	3.10	3.91	5.98
	height (m)	decrease –20%	5.09	8.69	6.55	5.17
		break without adjustment	5.09	8.93	6.86	5.20
		increase +20%	5.09	9.24	6.50	5.17
Adjusted full formulation time	width (m)	decrease –20%	413.48	160.21	282.47	477.86
		break without adjustment	399.65	154.64	269.09	369.41
		increase +20%	411.97	157.31	288.35	480.75
	velocity ($m \cdot s^{-1}$)	decrease –20%	6.44	4.45	2.08	6.06
		break without adjustment	5.67	4.69	3.15	3.48
		increase +20%	6.37	5.06	2.27	6.16
	height (m)	decrease –20%	5.93	9.58	7.92	5.24
		break without adjustment	5.09	8.93	6.86	4.93
		increase +20%	5.84	9.24	8.39	5.32
Adjusted breach width	width (m)	decrease –20%	410.22	152.71	264.13	474.35
		break without adjustment	399.65	154.64	269.09	476.63
		increase +20%	399.65	151.58	266.27	474.9
	velocity ($m \cdot s^{-1}$)	decrease –20%	6.29	6.16	3.74	5.92
		break without adjustment	5.67	4.69	3.15	6.03
		increase +20%	5.67	6.02	1.91	6.01
	height (m)	decrease –20%	5.73	8.71	6.47	5.14
		break without adjustment	5.09	8.93	6.86	4.93
		increase +20%	5.09	8.58	6.64	5.15

Source: own study.

Table 5. Dam break sensitivity analysis 2 (±50%)

Breach parameters	Flood parameters	Adjustments (±50%)	Hella	Khérenne	Chebla	Oueldja
Adjusted breach depth	width (m)	decrease –50%	399.65	153.51	272.67	475.52
		break without adjustment	399.65	154.64	269.09	476.63
		increase +50%	399.77	158.74	265.94	476.23
	velocity ($m \cdot s^{-1}$)	decrease –50%	5.67	4.56	2.24	5.98
		break without adjustment	5.67	4.69	3.15	6.03
		increase +50%	5.68	4.22	2.88	6.01
	height (m)	decrease –50%	5.09	8.80	7.14	5.17
		break without adjustment	5.09	8.93	6.86	5.20
		increase +50%	5.09	9.41	6.61	5.19
Adjusted full formulation time	width (m)	decrease –50%	413.06	157.63	269.34	477.32
		break without adjustment	399.65	154.64	269.09	369.41
		increase +50%	410.82	156.73	273.24	476.06
	velocity ($m \cdot s^{-1}$)	decrease –50%	6.42	4.86	4.13	6.05
		break without adjustment	5.67	4.69	3.15	3.48
		increase +50%	6.31	4.37	2.01	6.00
	height (m)	decrease –50%	5.90	9.28	6.88	5.22
		break without adjustment	5.09	8.93	6.86	4.93
		increase +50%	5.77	9.17	7.19	5.18
Adjusted breach width	width (m)	decrease –50%	411.87	159.01	269.66	478.18
		break without adjustment	399.65	154.64	269.09	476.63
		increase +50%	399.64	155.62	264.88	474.05
	velocity ($m \cdot s^{-1}$)	decrease –50%	6.36	4.58	4.10	6.07
		break without adjustment	5.67	4.69	3.15	6.03
		increase +50%	5.67	4.69	3.92	5.91
	height (m)	decrease –50%	5.83	9.44	6.90	5.24
		break without adjustment	5.09	8.93	6.86	4.93
		increase +50%	5.09	9.04	6.53	5.13

Source: own study.

and width and, slight change for height for the four locations Hella, Khérenne, Chebla and Oueldja. Obviously, all breach parameters have an influence either positive or negative on simulation results of the dam failure scenario by HEC-RAS model, and particularly for breach formation time adjustment which seems to be the most sensitive parameter. Adversely, other adjustments parameters have a weak impact on the model results.

Indeed, this simulation, which has been made with the four adjustments (±20 and +50) for three parameters, reveals that sensitivity analysis of the dam failure scenario is a very important step in the parameters evaluation which having a significant impact on the dam breakage and this could in the future to avoid and stop damages occurred by the dam failure.

CONCLUSIONS

The simulation of the Babar dam failure showed the formation of a flood wave, resulting in a sudden rise in water level downstream of the dam. This simulation allowed determining the characteristics of the submersion wave at all points of the valley; the height, the water velocity and the arrival time of the flood wave at sensitive points (villages, bridges, etc.). The selected breccia has a trapezoidal shape and was sized using the Froehlich formula, resulting in a maximum flow of 9253 $m^3 \cdot s^{-1}$. This made it possible to draw the risk map which shows the zones threatened by the submersion wave resulting from a complete failure of the structure. The maximum velocity can then be of the order of 26.5 $m \cdot s^{-1}$ which begins to attenuate from 27 km of the dam. The flood wave will arrive at the first village after 6:45 h while the last village will be hit after 8.45 h. This permits the organization of the warning system and the preventive evacuation riparian. This investigation highlighted that the hydraulic simulation by HEC RAS allows a visualization and a spatial analysis of the results such us the limits of the flood zones, the water levels of the flood…) and is therefore considered to be a decision-making tool by excellency for the flood risk management. The HEC RAS modelling is well fitted to help in carrying out dam failure analyses. The risk analysis associated with a dam rupture will help to develop contingency plans to help preventing the loss of human lives and property. This investigation presents the methodology used to interpret the dam failure scenario, as well as the available options. Problems of stability of the model are also addressed, besides the solution of some typical problems. With the sensitivity analysis, the breach parameters were confirmed such as the breach depth, formulation time, and breach width. These parameters have a great influence on the dam failure scenario, which can induce an elevation in the level of the flood wave downstream of the dam, and consequently a change in the limit of the risk zone.

REFERENCES

ACKERMAN C.T., BRUNNER G.W. 2012. Dam failure analysis using HEC-RAS and HEC-GeoRAS [online]. [Access 18.05.2017]. Available at: https://pdfs.semanticscholar.org/8b7a/16284061fe6a265ce3355414f7a38fcb9447.pdf

ANCY C. 2010. Hydraulique à surface libre [Free surface hydraulic]. Écublens, CH-1015 Lausanne. Laboratoire Hydraulique Environnementale, École Polytechnique de Lausanne pp. 234.

BARKAU R.L. 1982. Simulation of the July 1981 flood along the Salt River. Report for CE695BV, Special Problems in Hydraulics, Department of Civil Engineering, Colarado State University.

BERGHOUT A., MEDDI M. 2016. Sediment transport modelling in Wadi Chemora during flood flow events. Journal of Water and Land Development. No. 31 p. 23–31. DOI 10.1515/jwld-2016-0033.

BOUCHEHED H., MIHOUBI M.K., DERDOUS O., DJEMILI L. 2017. Evaluation of potential dam break flood risks of the cascade dams Mexa and Bougous (El Taref, Algeria). Journal of Water and Land Development. No. 33 p. 39–45. DOI 10.1515/jwld-2017-0017.

BOUSSEKINE M., DJEMILI L. 2016. Modelling approach for gravity dam break analysis. Journal of Water and Land Development. No. 30 p. 29–34. DOI 10.1515/jwld-2016-0018.

CHALFEN M., KOWALSKI J., MOLSKI T. 2005. Skuteczność rozwiązań technicznych chroniących tereny przyległe do stopni wodnych na przykładzie rejonu Malczyc [The efficiency of technical solutions for the protection of areas adjacent to a river dam – an example of the Malczyce region]. Woda-Środowisko-Obszary Wiejskie. T. 5. Z. 1 (13) p. 41–56.

CLAGUE J.J., EVANS S.G. 1994. Formation and failure of natural dams in the Canadian Cordillera. Bulletin / Geological Survey of Canada. 464. Ottawa. Geological Survey of Canada. ISBN 978-0660154961 pp. 35.

DERDOUS O., DJEMILI L., BOUCHEHED H., TACHI S.E. 2015. A GIS based approach for the prediction of the dam break flood hazard – A case study of Zardezas reservoir "Skikda, Algeria". Journal of Water and Land Development. No. 27 p. 15–20. DOI 10.1515/jwld-2015-0020.

DINCERGOK T. 2007. The role of dam safety in dam-break induced flood management. International Conference on River Basin Management. Kos. p. 683–691.

FROEHLICH D.C. 1995. Embankment dam breach parameters revisited. Water Resources Engineering. Proceedings of the 1995 ASCE Conference on Water Resources Engineering. San Antonio, Texas 14–18.08.1995 p. 887–891.

GAAGAI A. 2009. Étude hydrologique et hydrochimique du bassin versant du barrage de Babar sur Oued El Arab région est de l'Algérie [Hydrological and hydrochemical study of the Babar dam catchment area on Oued El Arab eastern region of Algeria]. Batna. University El Hadj Lakhdar pp. 117.

HU H.H., WALTON R. 2008. Advanced guidance on use of steady HEC-RAS. World Environmental and Water Resources Congress. Vol. 4. 12–16.05.2008. Honolulu, Hawaii, United States. p. 2028–2037. DOI 10.1061/40976(316)201.

LIGGETT J.A., CUNGE J.A. 1975. Numerical methods of solution of the unsteady flow equations. In: Unsteady flow in open channels. Vol. 1. Chapter 4. Eds. K. Mahmood, V. Yevjevich. Fort Collins, Co. Water Resources Publications p. 89–182.

MACDONALD T.C., LANGRIDGE-MONOPOLIS J. 1984. Breaching characteristics of dam failures. Journal of Hydraulic Engineering. Vol. 110. No. 5 p. 567–586. DOI 10.1061/(ASCE)0733-9429(1984)110:5(567).

MARCHE C. 2004. Barrages: crues de rupture et protection civile [Dams: flood failure and civil protection]. Presses inter Polytechnique. Canada. ISBN 978-2-553-01133-7 pp. 388.

MARCHE C. 2008. Barrages: crues de rupture et protection civile [Dams: flood failure and civil protection]. Presses inter

Polytechnique. 2nd edit. Canada. ISBN 978-2-553-01414-7 pp. 448.

MICHAEL G.D. 2010. Use of breach process models to estimate HEC-RAS dam breach parameters. 2nd Joint Federal Interagency Conference, Las Vegas, NV 27.06–1.07.2010 pp. 12.

MOKHTARI E.H., REMINI B., HAMOUDI S.A. 2016. Modelling of the rain–flow by hydrological modelling software system HEC-HMS – watershed's case of Wadi Cheliff-Ghrib, Algeria. Journal of Water and Land Development. No. 30 p. 87–100. DOI 10.1515/jwld-2016-0025.

SEMCHA A., MEKERTA B., TROALEN J.-P. 2008. Environmental consequences of the Algerian Fergoug's dam dredging. En: Insertion des grands ouvrages dans leur environnement. Journées nationales de géotechnique te de géologie de l'ingénieur JNGG'08 – Nantes [Environmental consequences of the Algerian Fergoug's dam dredging. In: Insertion of large civil engineering structures in the environment. Actes des journées scientifiques du LCPC. Vol. 1 p. 449–456.

SIMON N. 2015. Quantification des incertitudes et analyse de sensibilité pour codes de calcul à entrées fonctionnelles et dépendantes. PhD Thesis. Grenoble. Université de Grenoble pp. 176.

SINGH V.P. 1996. Dam breach modeling technology. Kluwer Academy Publishers. Dordrecht. ISBN 0-7923-3925-8 pp. 242.

SIRABAHENDA Z. 2012. Modélisation numérique du transport des sédiments en suspension dans une rivière en aménagement : Cas de la Rivière-Aux-Sables au Québec. MSc Thesis. École Polytechnique de Montréal pp. 90.

SMITH R.H. 1978. Development of a flood routing model for small meandering rivers. PhD Thesis. Rolla, MO. University of Missouri, Department of Civil Engineering pp. 159.

SWANSON F.J., OYAGI N., TOMINAGA M. 1986. Landslide dams in Japan. In: Landslide dams: Process, risk, and mitigation. Ed. R.L. Schuster. New York. American Society of Civil Engineers Special Publication. No. 3 p. 273–378.

USACE 1997. Engineering and design-hydrologic engineering requirements for reservoirs. Engineer manual. US Army Corps of Engineer. Military Bookshop. ISBN 1780397526 pp. 130.

USACE 2010. HEC-RAS. Hydraulic Reference Manual. Version 4.1 [online]. Davis, CA. Hydrologic Engineering Center, US Army Corps of Engineers. [Access 18.06.2018]. Available at: https://www.hec.usace.army.mil/software/hec-ras/documentation/HEC-RAS_4.1_Reference_Manual.pdf

VON THUN J.L., GILLETTE D.R. 1990. Guidance on breach parameters. Denver, Colorado. U.S. Bureau of Reclamation pp. 17.

WAHL T.L. 1998. Prediction of embankment dam breach parameters. A literature review and needs assessment. DSO-98-04 Dam Safety Research Report. U.S. Department of the Interior Bureau of Reclamation Dam Safety Office pp. 61.

WAHL T.L. 2004. Uncertainty of prediction of embankment dam breach parameters. Journal of Hydraulic Engineering. Vol. 130. No. 5 p. 389–397. DOI 10.1061/(ASCE)0733-9429(2004)130:5(389).